A Physical Channel Model for Nanoscale Neuro-Spike Communications

Eren Balevi, *Student Member*, and Ozgur B. Akan, *Senior Member, IEEE*

***Abstract*—Nanoscale communications is an appealing domain in nanotechnology. Novel nanoscale communications techniques are currently being devised inspired by some naturally existing phenomena such as the molecular communications governing cellular signaling mechanisms. Among these, neuro-spike communications, which governs the communications between neurons, is a vastly unexplored area. The ultimate goal of this paper is to accurately investigate nanoscale neuro-spike communications characteristics through the development of a realistic physical channel model between two neurons. The neuro-spike communications channel is analyzed based on the probability of error and delay in spike detection at the output. The derived communication theoretical channel model may help designing novel artificial nanoscale communications methods for the realization of future practical nanonetworks, which are the interconnections of nanomachines.**

***Index Terms*—Nanoscale communications, neuro-spike communications, physical channel model.**

I. Introduction

MOLECULAR communication is a completely new paradigm that can be used in nanonetworks, i.e., the interconnections of nanomachines [1], [11], [17]. It provides communication using molecules as an information carrier such as calcium signaling, molecular motors, pheromones, neurotransmitters as stated in [7], [10], [12], [15]. Among all molecular communication paradigms, neuro-spike communications, which use the neurotransmitters as information carriers, is a vastly unexplored communication paradigm.

Neuro-spike communications occurs between neurons where the transmission is done by electro-chemical impulses and neurotransmitters. It is a hybrid model that includes both the transmission of impulses and molecular communication of neurotransmitters.

The performance of neuro-spike communications is quite good in terms of reliability, speed and robustness [4]. In this manner, a realistic physical channel model of neuro-spike communications is substantially needed to be able to completely characterize its fundamental properties. Neuroscience and medicine may benefit from the model in the future. Moreover, this model can be used to derive new nanoscale communications methods.

Manuscript received May 10, 2011; revised October 23, 2011. The associate editor coordinating the review of this paper and approving it for publication was M.-S. Alouini.

This work was supported in part by the Turkish Scientific and Technical Research Council under grant #109E257, by the Turkish National Academy of Sciences Distinguished Young Scientist Award Program (TUBA-GEBIP), and by IBM through IBM Faculty Award.

The authors are with the Next-Generation and Wireless Communications Laboratory (NWCL), Department of Electrical and Electronics Engineering, Koc University, Istanbul, 34450, Turkey (e-mail: erenbalevi@gmail.com, akan@ku.edu.tr).

Digital Object Identifier 10.1109/TCOMM.2012.010213.110093

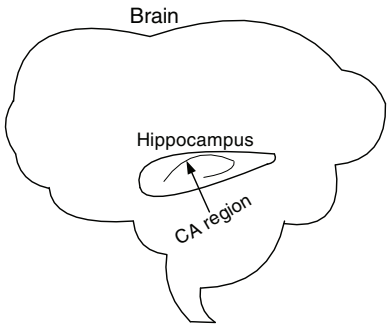

Fig. 1. CA region in the hippocampus location of the brain.

Neuro-spike communications may show some differences due to the various types of neurons. Although neurons have different firing rates, types of neurotransmitters and receptors, the communication of neurons at Cornu Ammonis (CA) region, a special area in the hippocampus location of the brain, is chosen for our modeling. This region is shown in Fig. 1 and the physical communication channel is modeled according to the properties of these neurons.

The reasons for choosing to analyze the CA region are as follows. These neurons are heavily investigated in physiology, and hence, there exist many experimental results which reveal their properties. Furthermore, it is responsible of critical functions like memory in the brain.

There are several studies about the physiological principles of these neurons. The axonal propagation in the hippocampal CA3 neurons and how reliable the axonal transmission occurs in this location are investigated in [16], [18]. In case of transmission that occurs at synapses, the vesicle release function of the hippocampal neurons is described related to some synaptic concepts in [6], [20], [21]. Trial-to-trial variability in synapses is explained by making some experiments and interpreting their results in [2], [14]. However, none of these works deals with the communication behaviors of neurons as a new nanoscale communications paradigm and models the end-to-end neural communications channel.

A synaptic model is proposed in [13]. The model shows that redundancy of synapses improves the efficiency of information transmission. However, this model does not cover the use-dependent change of neurons, i.e., the change in the behavior of the channel from one usage to the other, which is called plasticity. Moreover, the diffusion of neurotransmitters in the synapse is not considered. Furthermore, the effects of different type of receptors are not taken into account on the Excitatory

PostSynaptic Potential (EPSP) generation. These shortcomings deviate the synaptic channel model from the realistic neural behavior.

The objective of this paper is to derive a realistic physical channel model of nanoscale neuro-spike communications between one input and one output neuron by using the fundamental features of the communication theory. For this purpose, first, neuro-spike communications is expressed by dividing it into basic building blocks. After that, each block is investigated in detail in order to model it in terms of the fundamental communication theory. Eventually, the modeling of each neuro-spike basic block yields a complete channel model. In this work, the input-output analysis of the modeled channel is performed.

The remainder of this paper is organized as follows. In Section II, the fundamental features of the neuro-spike communications are given. Section III, IV, and V focus on the details of this communication paradigm. Based on this, the physical channel model is given and its analysis is performed in Section VI. The numerical results are shown in Section VII. The paper is finalized with the concluding remarks in Section VIII.

II. Neuro-Spike Communications

A neuron is composed of three main parts which are the soma, the axon and the dendrites. The soma is responsible for the spike generation in response to stimuli, the axon is the place where the spikes are conducted and the dendrites function is the reception of the excitation.

Spikes or impulses are used to transmit information from one neuron to another. Hence, it is called neuro-spike communications, shown in Fig. 2. It can be divided into three main parts. The first one, the *axonal transmission*, is the propagation of the spikes along the axon. At the end of the axon, there are some specialized terminals, which are called the presynaptic terminals whose function is the release of neurotransmitter packets or vesicles to the gaps among neurons, i.e., synapses. The release depends on the plasticity of the neuron, i.e., the change in the release probability in response to its history. Release of the packets to the synapses initiates the *synaptic transmission*, which is the second main part of the neuro-spike communications. Since each packet contains many neurotransmitter molecules, following the release the neurotransmitters inside the packets go out and the diffusion of each neurotransmitter begins towards the output neuron. In order to get the diffused molecules, the neurons have many postsynaptic terminals at the dendrite in which the receptors are located. There are two main types of the receptors, which are the ionotropic and the metabotropic receptors. The difference between them is that the ionotropic receptors directly excite the neurons, whereas the metabotropic receptors have indirect effect such that they initiate the metabolic change in the neuron, and this change excites the neuron. At the end of the diffusion, these neurotransmitters bind to the receptors at the postsynaptic terminal. When neurotransmitters bind to the receptors, the movement of ions begins, which provides excitation, and this constitutes the last part of the communications called *spike generation*. Moving ions excite the membrane potential of the output neuron, and lead to the EPSP generation. The level of excitation changes from one packet to another, because of the variation in the behavior of neurons with time, which is called the *trial-to-trial variability*. Since neurons have some threshold value to be depolarized, the excitation level must be above the threshold. However, one receptor is not sufficient to depolarize the neuron, therefore, the response of the group of the receptors belonging to the same neuron are summed. If the total summation is greater than the threshold value, the neuron has sufficiently depolarized and the spike is generated at the output, which completes the information transfer.

One example of the neuro-spike communications is present at the CA region. The block diagram of the spike communications between the input neuron and the output neuron at CA region is given in Fig. 3. It covers the axonal transmission, the fundamental physiological events during the synaptic transmission, which are the vesicle release of the neuron in response to a spike, the diffusion, the EPSP due to the vesicle release and the trial-to-trial variability of this potential, generation of spikes at the output and the noise, which is generated during the axonal and synaptic transmission.

III. Neuro-Spike Communications: Axonal Transmission

An experiment on the axonal transmission in the CA region of rat's brain reveals that for low frequency firing rate, spikes propagate through the axon without any amplitude distortion, and nearly no failure occurs [18]. On the other hand, for high frequency firing rate, if the inter-spike interval diminishes, the amplitude of the consecutive spikes decreases logarithmically. Moreover, spikes time-delay rises with increasing spike frequency.

It is deduced from the results of this experiment that the axon can be modeled as a modified version of a second order Butterworth filter. The filter is modified, because the magnitude response jumps to zero, which is the consequence of the gap time between two consecutive spikes, called refractory period. Its normalized sample transfer function is given as

$$H(jw) = \frac{a}{(-w^2 + jbw + a)}[u(jw) - u(jw - c)] \quad (1)$$

where $u(.)$ is the unit step function. The values of filter coefficients a, b, c are not critical for our purpose and may be determined with respect to the experiment in [18].

There is a functional similarity between the low pass anti-aliasing filter and the axonal filter that achieves the elimination of the spikes which has smaller inter-spike intervals.

In the physical channel model, the axonal transmission is implemented as follows. Firstly, the impulse train is converted into rectangular pulses such that when an impulse comes, the pulse level goes high assuming the pulse is initially in low state. It remains there until the next impulse and goes to low state for the next incoming impulse. It repeats the same procedure for all impulses. Secondly, these rectangular pulses pass through the anti-aliasing filter, and lastly, pulses are converted into impulses again. The main rationale behind the state transition between impulses and rectangular pulses is to filter the impulses having lower inter-spike intervals by the anti-aliasing filter. This part is shown in Fig. 4(a).

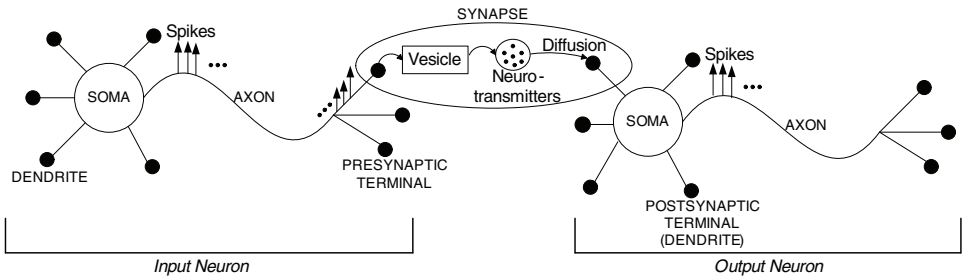

Fig. 2. Neuro-spike communications.

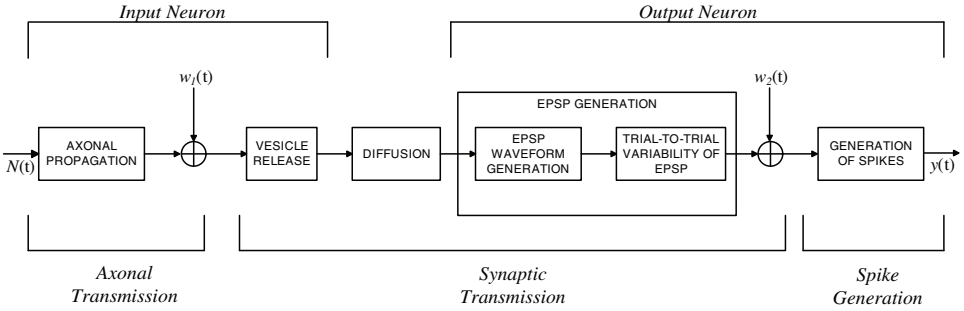

Fig. 3. Block diagram of the neuro-spike communications.

IV. Neuro-Spike Communications: Synaptic Transmission

Synaptic transmission is composed of three parts, namely the vesicle release, the diffusion and the EPSP generation.

A. Vesicle Release

The released neurotransmitter packets are called *vesicles* or *quanta*. They are secreted in special areas of the presynaptic terminals called active zones. There are two important definitions related with the quanta, the first one is the quantal content that is the average number of quanta generated in response to a spike. The majority of neurons located at the hippocampus have one single active zone per presynaptic terminal [20]. Furthermore, hippocampal pyramidal neurons release one or zero quanta from a single active zone in response to an incoming spike [21]. The second one is the quantal size or quantal amplitude that is the synaptic response to a single quanta. The quantal size of hippocampal CA neurons is not constant and varies from quanta to quanta. This leads to the amplitude fluctuations at the output neuron, which is discussed in Section IV-C.

Vesicle release has a random nature. Even if a spike comes to a presynaptic terminal, a vesicle may not be generated. Conversely, if a spike does not come, a vesicle may be generated spontaneously. However, the probability of spontaneously occurred vesicle is very low for hippocampal neurons [13], therefore, it can be ignored.

The short term synaptic plasticity that occurs in a few seconds takes an important role in the vesicle release probability. If the initial release probability is lower and stimuli trains come, firstly, the response increases due to the facilitation, defined as the ease of release, and then, decreases due to the depletion, i.e., difficulty of release [6]. Since the initial release probability of hippocampal neurons is low, it exhibits this behavior [3].

The vesicle release function of the neuro-spike communications is represented as packet release probability depending on the inter-spike interval, γ, and the channel state, S, in the physical channel model shown in Fig. 4(b).

B. Diffusion

Once a vesicle is released, several neurotransmitters included in the vesicle diffuse through the synapse. This behavior is considered as diffusive propagation in the physical channel model shown in Fig. 4(c). Whether a diffused neurotransmitter can excite a potential on the output or not depends on the receptors status, because they may not be ready for excitation. This issue is further investigated in Section IV-C.

C. EPSP Generation

Diffused neurotransmitters affect the output neuron via the receptors present on its extremity. There are two main types of receptors on the output neuron, namely, the ionotropic receptors, Alpha-Amino-3-Hydroxy-5-Methyl-4-Isoxazole-propionate (AMPA) and N-Methyl-D-Aspartate (NMDA), and the other is the metabotropic receptors, mGluRs.

The normalized analog voltage waveform generated at one receptor in response to a neurotransmitter is an alpha function such that [4], [19]

$$\alpha(t) = \frac{t}{\tau} exp(1 - \frac{t}{\tau}) u(t) \tag{2}$$

where τ is some constant associated with the type of the receptor. The corresponding alpha functions for AMPA, NMDA, mGluR type receptors are $\alpha_A(t)$, $\alpha_N(t)$, $\alpha_m(t)$ with $\tau = \tau_1$, $\tau = \tau_2$, $\tau = \tau_3$, respectively and $\tau_3 \gg \tau_2 > \tau_1$.

Each neurotransmitter generates a voltage waveform at the receptors as in (2) and a continuous analog signal is formed during the transmission of spikes. Therefore, the generation of EPSP waveform from the neurotransmitters will be modeled as a modulator in the physical channel model illustrated in Fig. 4(d).

The magnitude of the response depends on some factors. These are: the quantal size of each vesicle, the binding probability of the diffused neurotransmitters to the receptors, the state and number of available receptors. Since they all have random nature, there is a trial-to-trial variability in the response to a single vesicle, where trial refers to the excitation level due to the vesicle release [2].

In the physical channel model, trial-to-trial variability of the amplitude is implemented as random amplitude distortion block as illustrated in Fig. 4(e).

V. Neuro-Spike Communications: Noise Components and Spike Generation

There are two major sources of noise in neuro-spike communications. One is due to the axon, i.e., the axonal noise and the other is due to the synapse, i.e., the synaptic noise.

Channel noise is the most dominant axonal noise source [13]. It stems from the stochastic opening and closing of voltage gated ion channels which are activated by potential difference and allow the movement of ions through the neuron [5]. In case of the channel noise, spontaneous spike occurs depending on the randomly opening of the Na^+ channels that are the voltage gated ion channels located at neuron membrane and independent of the type of the axon [8].

The noise in the synapse and the dendrites, where the postsynaptic terminal is located, constitutes the synaptic noise. The basic source of the synaptic noise is the background synaptic activity which is due to the multiple access of synapses from thousands of other synapses [9], [13].

Synaptic background noise covers the effect of many different synapses. Since each synaptic effect has the same random nature, their sum follows a probability distribution function that converges to Gaussian due to the central limit theorem. Hence, synaptic noise is modeled as a Gaussian process.

In order to fire a spike at the output, it has to be sufficiently depolarized, i.e., it exceeds the threshold level of the neuron to fire a spike. However, one active receptor is not sufficient to form a spike. Therefore, a spike is formed by the group of active receptors' responses in the same postsynaptic terminal in two ways. The first one is the temporal summation which occurs due to the effect of neurotransmitters released from the same presynaptic terminal to the same postsynaptic terminal with different arrivals times. Since each vesicle contains many neurotransmitters, the arrival of them may be in different times. The second is the spatial summation which corresponds to the effect of the different presynaptic terminals on the same postsynaptic terminal. In the physical channel model, the spatial summation does not have any effect because the channel is modeled between only one presynaptic and postsynaptic terminal.

The spike generation block of neuro-spike communications is realized with the receiver shown in Fig. 4(f).

VI. Analysis of the Physical Channel Model

An input neuron has many presynaptic terminals, which means that it leads to the excitation in many postsynaptic terminals. However, we consider the channel between one single input neuron axon, one single presynaptic terminal of the input neuron and one single postsynaptic terminal of the output neuron. Therefore, it can be classified as a Single Input Single Output (SISO) channel. It involves all the steps from the transmission of impulses along the input neuron axon until the generation of impulses at the output neuron. This SISO channel is modeled in Fig. 4, where each block represents the major functionality of the neuro-spike communications.

In this part, we specify the input-output relation of the channel by deriving the input impulse train detection probability at the output and the channel delay.

A. Input-Output Relation of the Channel

Any excitation above the threshold level of the input neuron at the CA region generates impulses at the neuron axon. The arrival of this excitation to the input neuron is a stochastic process. Since there may be numerous independent sources that produce the excitation, this stochastic model can be considered as a Poisson process. Furthermore, the arrival of the stimuli can result no impulse, one impulse or more than one impulse independent of time, therefore, the firing rate of the neuron is itself a stochastic process as well. This does not resemble the classical Poisson process with deterministic intensity. In this case, the intensity is random. This process is called doubly stochastic Poisson process.

In order to obtain the realistic neuro-spike communications, the modeled channel input is taken as impulse train consistent with the doubly stochastic Poisson process similar to the input of the neuron. Eventually, the input of the channel is a random process $N(t)$ where $\{N(t), [0,T]\}$ is a point process. It is a doubly stochastic Poisson process with a non-negative random intensity, λ_n.

The channel input is given by

$$N(t) = \sum_k \delta(t - t_k) \tag{3}$$

The probability of an impulse train having i impulses in $[0,T]$ is defined as $P(\hat{N(T)} = i)$.

The signal in the presynaptic terminal of the input neuron, $q(t)$ is

$$q(t) = N_a(t) + w_1(t) \tag{4}$$

where $N_a(t)$ is the output of the anti-aliasing filter, and $w_1(t)$ is the axonal noise such that $w_1(t) = \delta(t - t_m)$.

It is unlikely that the axonal noise generates a spike in the limited time interval, $[0,T]$, therefore, we assume that at most one erroneous spike occurs due to the axonal noise.

Since the axonal noise mainly results from the stochastic opening of the ion channels irrespective of the input impulse train propagating along the axon, the spike due to the axonal noise is independent of the actual input. Therefore, $N_a(t)$ and $w_1(t)$ are independent processes.

$q(t)$ can also be expressed as follows

$$q(t) = \sum_i q_i(t) \tag{5}$$

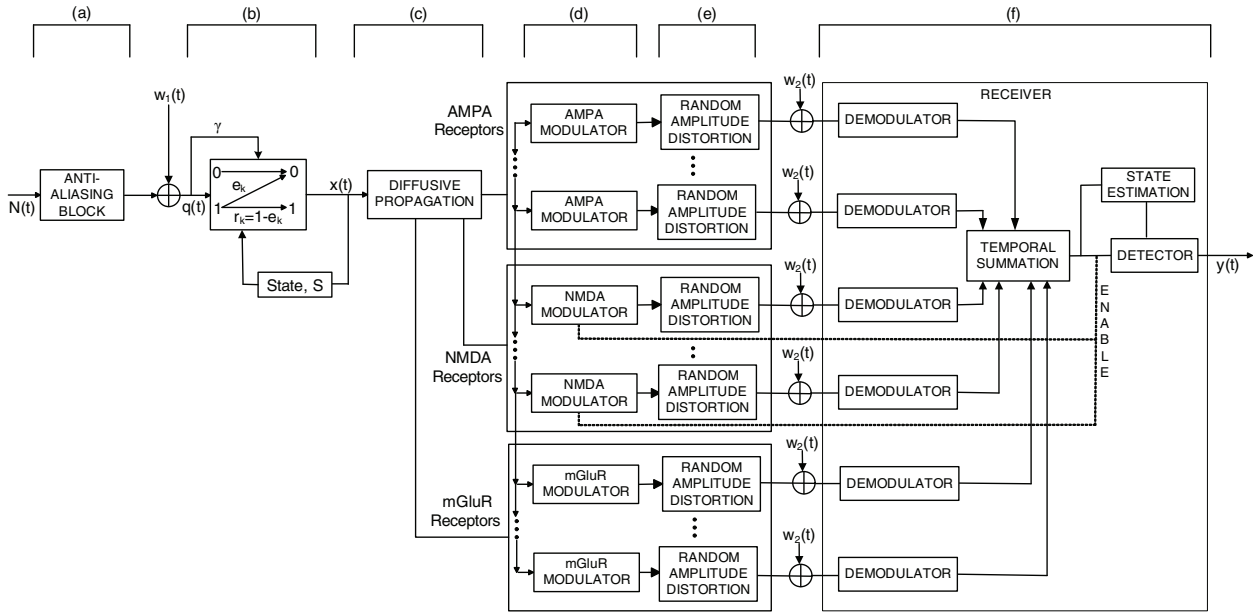

Fig. 4. The physical channel model of a neuro-spike communications channel.

where $q_n(t) \propto \delta(t - t_n)$ which is taken as the n^{th} impulse, q_n, in the packet generation mechanism.

The probability of an impulse train having i impulses at $q(t)$ in $[0, T]$ is

$$P(q(t) = i) = P(N\hat{(T)} = i - 1)P_a + P(N\hat{(T)} = i)(1 - P_a) \tag{6}$$

where P_a is the probability of an impulse occurrence due to the axonal noise.

We observe the effect of any impulse $q(t)$, at the output, $y(t)$ by dividing the channel into 3 sub-portions, namely, the packet generation mechanism, the synapse and the receiver.

1) Packet Generation Mechanism: Each input q_n and each output x_n have a binary alphabet such that 1 denotes the incoming impulse for the input and released packet for the output, whereas 0 symbolizes no impulse for the input and no released packet at the output. The vesicle release probability, r_k, between each impulse q_n and each packet x_n mainly depends on the inter-spike interval, γ and the channel state, S. γ can be extracted from the input by keeping the previous spike time and the state information, S, is given to the output from a feedback path.

According to the usage of channel, there exist a finite number of, i.e., $l + 1$, different channel states, $S = \{s_0, s_1, s_2, ..., s_l\}$ where s_0 corresponds to an initial state, s_l corresponds to no release, i.e., $r_k = 0$, and the intermediate states are for different release probability of the channel.

The state transitions are stationary and depend only on the previous state. Thus, $\{s_n, n = 0, 1, 2, ...\}$ is a stationary Markov process.

The packet generation structure is the combination of $l + 1$ channels having different states and release probabilities with the same input and output alphabet for a specific γ. This binary input binary output alphabet finite state channel with Markov transitions is called Finite State Markov Channel (FSMC) [22].

The transition matrix of FSMC is denoted as **T** and the error matrix, which is the non-transmission of the incoming impulse for all γ and S, is **e** such that

$$e_k = \int_0^\infty \sum_n P(x_n = 0 | q_n = 1, s_k, \gamma) P(S = s_k) f_\gamma(\gamma) d\gamma \tag{7}$$

and $f_\gamma(\gamma)$ is the probability density function of the γ.

Hence, the release probability is $r_k = 1 - e_k$.

2) Synapse: After the release of the packet to the synapse, the issue is the excitation of a potential at the output by this packet. Any released packet, x, can be considered as a $[1\ x\ j]$ matrix assuming one packet includes j neurotransmitters and it can be divided into j independent $[1\ x\ 1]$ matrices, x_i. Since, each packet has finite number of identical tiny neurotransmitters, for the sake of simplicity they can be treated as point sources at R whose initial position is R_i such that $x_i = \delta(R - R_i)$.

Assuming that the diffusion occurs in homogeneous medium at 1 dimension, the diffusion of each particle x_i at point R_i at time t is solved by the Green's function that exhibits the Gaussian diffusion in response to a particle release. x_i diffuses through the synapse to the target neuron. The neurotransmitter that arrives to the target neuron x_i^d is written as

$$x_i^d = \int \delta(R - R_i) G(R_i^f - R_i, t) dR_i = \frac{1}{\sqrt{4\pi t}} exp(\frac{-(R_i^f - R_i)^2}{4t}) \tag{8}$$

where R_i^f is the destination position of the particle.

If a packet is released successfully from the presynaptic terminal, the probability density function of the arrival of incoming neurotransmitter at time θ_i is

$$f_{\theta_i}(\theta_i) = \frac{a}{\sqrt{4\pi\theta_i}} exp(\frac{-b^2}{4\theta_i}) \tag{9}$$

where b is equal to $(R_i^f - R_i)$ and a is any constant that satisfies $\int_{-\infty}^{\infty} f_{\theta_i}(\theta_i) d\theta_i = 1$.

Neurotransmitters present in one packet affect many receptors. The AMPA and the NMDA are the main receptors that

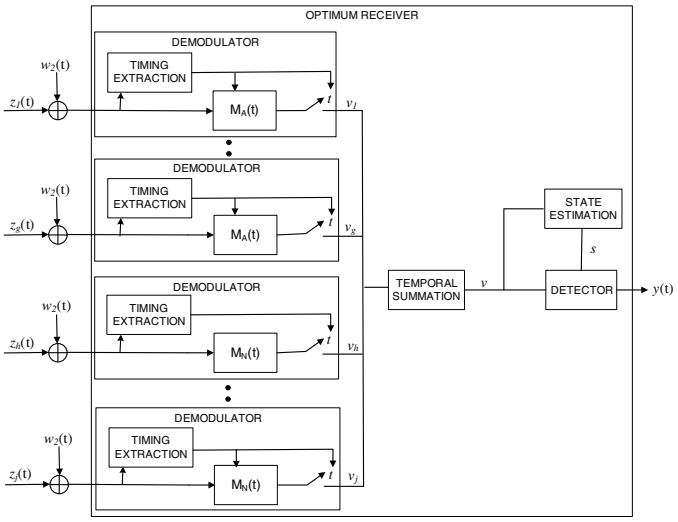

Fig. 5. Optimum receiver of neuro-spike communications channel.

provide the excitation [4]. Therefore, mGluRs can be neglected and we assume that neurotransmitters from x_1 to x_g affect the AMPA receptors, and neurotransmitters from x_h to x_j affect the NMDA receptors.

When the neurotransmitters affect the AMPA receptors, they are modulated by an AMPA modulator. Its signal waveform is given in (2). The AMPA modulated signal in response to one neurotransmitter is subject to the random amplitude distortion [13]. Hence,

$$z_i(t) = d_i \alpha_A(t - \theta_i),\ 1 \leq i \leq g \tag{10}$$

where d_i is a random variable due to the random amplitude distortion stemming from the trial-to-trial variability in neurons and g is any arbitrary value.

The modulation of the neurotransmitters in the NMDA receptors are different than the AMPA. The activation of the NMDA receptors depend on the long term plasticity or Long Term Potentiation (LTP) [23]. LTP is the intrinsic behavior of a neuron that provides the amplification of the signal transmission in the long time. Unlike the AMPA receptors, some activation time is required for the NMDA receptors. Thus, the waveform is shifted by $t_0 > 0$. Therefore,

$$z_i(t) = d_i \alpha_N(t - t_0 - \theta_i), h \leq i \leq j \tag{11}$$

where $h = g + 1$.

3) Receiver: Receiving structure of a neuron is not known exactly, therefore, we design the optimum receiver for this channel model. The block diagram of the optimum receiver is given in Fig. 5.

The input of the receiver for any released packet in the time interval between T_n and T_{n+1} is,

$$v_i(t) = z_i(t) + w_2(t), 1 \leq i \leq j \tag{12}$$

where $w_2(t)$ is white Gaussian noise, because synaptic noise occurs due to various independent sources [13]. Hence, they are independent from each other.

$z_i(t)$ has random time delay, θ_i, therefore, it must be extracted before filtering.

Matched filter maximizes the signal-to-noise ratio (SNR) for additive white Gaussian noise (AWGN). Two types of matched filters are used for AMPA and NMDA modulators, namely $M_A(t)$ and $M_N(t)$ respectively. They are,

$$M_A(t) = \alpha_A(T_{n+1} - t + \theta_i), T_n \leq t \leq T_{n+1} \tag{13}$$

$$M_N(t) = \alpha_N(T_{n+1} - t + t_0 + \theta_i), T_n \leq t \leq T_{n+1} \tag{14}$$

The output of the matched filter pertaining to the AMPA modulator for $T_n \leq t \leq T_{n+1}$ and $1 \leq i \leq g$ is

$$\begin{aligned} v_i &= \int_{T_n}^{T_{n+1}} d_i \alpha_A(\tau - \theta_i)\alpha_A(T_{n+1} - t + \theta_i + \tau)d\tau \\ &\quad + \int_{T_n}^{T_{n+1}} w_2(\tau)\alpha_A(T_{n+1} - t + \theta_i + \tau)d\tau \end{aligned} \tag{15}$$

The output of the matched filter of the NMDA modulator for $T_n \leq t \leq T_{n+1}$ and $h \leq i \leq j$ is

$$\begin{aligned} v_i &= \int_{T_n}^{T_{n+1}} d_i \alpha_N(\tau - t_0 - \theta_i)\alpha_N(T_{n+1} - t + t_0 + \theta_i + \tau)d\tau \\ &\quad + \int_{T_n}^{T_{n+1}} w_2(\tau)\alpha_N(T_{n+1} - t + t_0 + \theta_i + \tau)d\tau \end{aligned} \tag{16}$$

Each d_i and noise component are independent identically distributed (i.i.d.). Moreover, they are independent from each other.

After the temporal summation, v becomes

$$v = \sum_{i=1}^{j} v_i \tag{17}$$

Furthermore, the state estimation is needed to make a decision. We show that it can be calculated recursively at the output.

The current channel state, s_n is found recursively by using the previous output of the matched filters, v^{n-1}, and the previous states, s^{n-1}, such that it is expressed by using conditional probability property as

$$P(s_n|v^{n-1}, s^{n-1}) = \frac{P(v_{n-1}, s_n|v^{n-2}, s^{n-1})P(v^{n-2}, s^{n-1})}{P(v^{n-1}, s^{n-1})} \tag{18}$$

It can be expanded by detailing the first term of the numerator as

$$\begin{aligned} P(s_n|v^{n-1}, s^{n-1}) &= \frac{P(s_n|v^{n-2}, s^{n-1})P(v^{n-2}, s^{n-1})}{P(v^{n-1}, s^{n-1})} \times \\ &\quad P(v_{n-1}|v^{n-2}, s_n, s^{n-1}) \end{aligned} \tag{19}$$

Since v does not depend on the next channel state, the first term of the numerator is converted to

$$P(v_{n-1}|v^{n-2}, s_n, s^{n-1}) = P(v_{n-1}|v^{n-2}, s^{n-1}) \tag{20}$$

The current channel state only depends on the previous state and the previous output of the matched filters, therefore, the second term of the numerator in (19) is simplified to

$$P(s_n|v^{n-2}, s^{n-1}) = P(s_n|s_{n-1}) \tag{21}$$

From the stationarity property of the state transitions, $P(s_n|s_{n-1}) = \mathbf{T}$,

$$P(s_n|v^{n-1}, s^{n-1}) = \frac{P(v_{n-1}|v^{n-2}, s^{n-1})\mathbf{T}P(v^{n-2}, s^{n-1})}{P(v^{n-1}, s^{n-1})} \tag{22}$$

The denominator of (22) be written by using conditional probability property as

$$P(v^{n-1}, s^{n-1}) = P(s^{n-1}|v^{n-1})P(v^{n-1}) \tag{23}$$

$P(s^{n-1}|v^{n-1})$ can be expressed by considering the current channel state only depends on the previous state and the previous output such that

$$P(s^{n-1}|v^{n-1}) = P(s_0)P(s_1|v_0, s_0)\cdots P(s_{n-1}|v^{n-2}, s^{n-2}) \tag{24}$$

Therefore,

$$P(s_n|v^{n-1}, s^{n-1}) = \frac{P(v_{n-1}|v^{n-2}, s^{n-1})\mathbf{T}P(v^{n-2}, s^{n-1})}{P(s_0)\prod_{i=1}^{n-2} P(s_i|v_{i-1}, s_{i-1})P(s_{n-1}|v^{n-2}, s^{n-2})P(v^{n-1})} \tag{25}$$

Hence, the current state is recursively calculated from the previous state.

Since the current state is probabilistically known, we prefer a single packet decision instead of a group decision as a design criterion.

There are two hypotheses for each packet decision such that

$$H_1 : v = \sum_i c_i d_i + n_i, 1 \le i \le j \tag{26}$$

$$H_0 : v = \sum_i n_i, 1 \le i \le j \tag{27}$$

where c_i and n_i for $1 \le i \le g$ are

$$c_i = \int_{T_n}^{T_{n+1}} \alpha_A(\tau - \theta_i)\alpha_A(T_{n+1} - t + \theta_i + \tau)d\tau \tag{28}$$

$$n_i = \int_{T_n}^{T_{n+1}} w_2(\tau)\alpha_A(T_{n+1} - t + \theta_i + \tau)d\tau \tag{29}$$

and for $h \le i \le j$ are

$$c_i = \int_{T_n}^{T_{n+1}} \alpha_N(\tau - t_0 - \theta_i)\alpha_N(T_{n+1} - t + t_0 + \theta_i + \tau)d\tau \tag{30}$$

$$n_i = \int_{T_n}^{T_{n+1}} w_2(\tau)\alpha_N(T_{n+1} - t + t_0 + \theta_i + \tau)d\tau \tag{31}$$

The threshold value, Ω for the decision rule is found by Neyman-Pearson method such that

$$\Omega = \frac{P(v|H_1)}{P(v|H_0)} \tag{32}$$

Since $(v|H_1)$ is the sum of many i.i.d. random variables, it is Gaussian due to the central limit theorem. Its mean and variance are

$$E[v|H_1] = \sum_i c_i E[d_i] = \mu \tag{33}$$

$$Var[v|H_1] = \sum_i c_i^2 Var[d_i] + Var[n_i] = \sigma_1^2 \tag{34}$$

Similarly, $(v|H_0)$ is Gaussian as well with the following mean and variance

$$E[v|H_0] = 0 \tag{35}$$

$$Var[v|H_0] = \sum_i Var[n_i] = \sigma_0^2 \tag{36}$$

Hence, the decision threshold, Ω, is

$$\Omega = \frac{\frac{1}{\sqrt{2\pi\sigma_1^2}} exp(-\frac{(v-\mu)^2}{2\sigma_1^2})}{\frac{1}{\sqrt{2\pi\sigma_0^2}} exp(-\frac{v^2}{2\sigma_0^2})} \tag{37}$$

The threshold value and sufficient statistics are expressed as,

$$th = \ln\Omega - \ln\frac{\sigma_0}{\sigma_1} + \frac{\mu^2}{2\sigma_1^2} \tag{38}$$

where th is the threshold value

$$y = v^2(\frac{1}{2\sigma_0^2} - \frac{1}{2\sigma_1^2}) + v(\frac{\mu}{\sigma_1^2}) \tag{39}$$

and y is the sufficient statistics.

The optimum decision is based on the minimum probability of error, P_b, depending on current channel state and expressed by

$$P_b = P(y = 0|q = 1)P(q = 1) + P(y = 1|q = 0)P(q = 0) \tag{40}$$

P_b can also be written in terms of x, i.e.,

$$\begin{aligned} P_b &= P(y = 0|x)P(x|q = 1)P(q = 1) \\ &\quad + P(y = 1|x)P(x|q = 0)P(q = 0) \end{aligned} \tag{41}$$

which can be rewritten as

$$\begin{aligned} P_b &= [P(y = 0|x = 0)e_k + P(y = 0|x = 1)r_k]P(q = 1) \\ &\quad + P(y = 1|x = 0)P(q = 0) \end{aligned} \tag{42}$$

where

$$\begin{aligned} P(y = 0|x = 0) &= P(y < th|x = 0) \\ P(y = 0|x = 1) &= P(y < th|x = 1) \\ P(y = 1|x = 0) &= P(y > th|x = 0) \end{aligned} \tag{43}$$

Therefore, the probability of error, P_b, is

$$\begin{aligned} P_b &= [P(y < th|x = 0)e_k + P(y < th|x = 1)r_k] \\ &\quad P(q = 1) + P(y > th|x = 0)P(q = 0) \end{aligned} \tag{44}$$

The output, $y(t)$, is a point process as well as $N(t)$. The probability of impulse train at $y(t)$ due to $q(t)$ having i impulses, found in (6), is

$$P(y(t) = i) = (1 - P_b)^i \tag{45}$$

Moreover, the average impulse transmission rate, I_r, can be expressed by

$$I_r = \sum_i P(\hat{N(T)} = i)(1 - P_b)^i \tag{46}$$

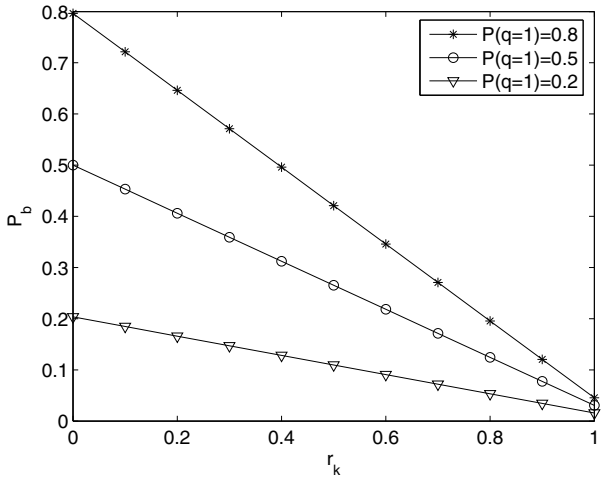

Fig. 6. The effect of the probability of incoming impulse to the presynaptic terminal.

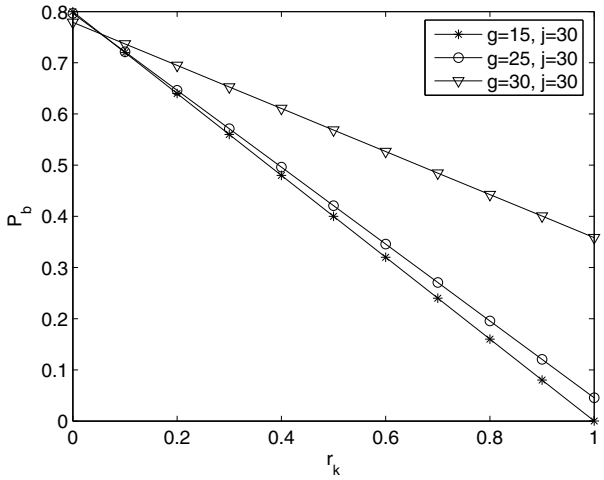

Fig. 7. The effect of number of g and j on the channel performance.

B. The Channel Delay

The channel delay brings some latency for the transmission of each impulse. It is equal to the sum of the delay while propagating through the axon of the input neuron and random diffusion time, θ_i, at synapse. The delay due to the axon can be found using the transfer function in (1), and random diffusion time is calculated via its probability density function found in (9). Eventually, each impulse at $y(t)$ incurs in latency with respect to $N(t)$.

VII. Numerical Analysis

The main performance measure of the channel is the probability of impulse error, P_b. The lower P_b, the more efficient the channel we obtain. Hence, we observe the error probability at the output. In addition to that, the channel delay is observed.

A. Probabilistic Analysis of Impulse Detection

Our aim is to show the effect of the probability of incoming impulse to the presynaptic terminal, $P(q = 1)$, the total number of affected AMPA, g, and NMDA receptors, $(j - g)$, the total synaptic noise, V_T, the threshold value of the output neuron, ω, and the expected value of random variable d_i on P_b.

The variance of d_i is not observed, because high or low variance of d_i is not significantly changed the P_b and delay.

Unless otherwise stated, the channel parameters are fixed to some arbitrarily chosen values as shown in Table I where V_T is

$$V_T = \sum_i Var[n_i] \tag{47}$$

To prevent any interference between consecutive symbols, T_{n+1} is taken as 100 unit time which is much greater than the values of τ_1 and τ_2 which determine the duration of the symbol response time.

Since $(\frac{1}{2\sigma_0^2} - \frac{1}{2\sigma_1^2}) << \frac{\mu}{\sigma_1^2}$, the sufficient statistics in (39) is reduced to

$$y = v(\frac{\mu}{\sigma_1^2}) \tag{48}$$

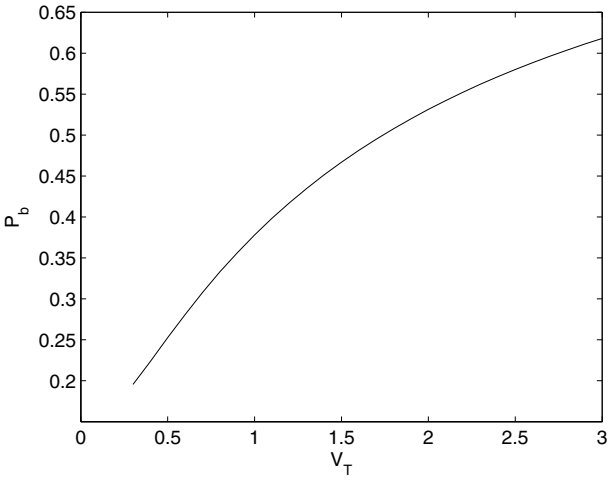

Fig. 8. The effect of noise on the channel performance with $r_k = 0.8$.

and the calculations are performed accordingly.

In Fig. 6, the effect of the probability of incoming impulse to the presynaptic terminal is illustrated. High impulse probability leads to increase in P_b. Fig. 6 verifies the short term plasticity such that P_b increases when the probability of incoming impulse rises.

Fig. 7 reveals the importance of the NMDA receptors. When the NMDA receptors are active, i.e., $(j - g) \neq 0$, the channel performance improves. This result is compatible with the long term plasticity in neurons, which means the amplification in the signal transmission quality relies on the activation of the NMDA receptors.

The synaptic noise is observed in Fig. 8. An increase in the power of noise degrades the effect of the neurotransmitters at the output receptors. Therefore, the input impulse may not be detected or an erroneous impulse is generated due to noise. Both of them lead to poor channel performance.

In Fig. 9, the effect of ω on the channel performance is investigated. Although an increase in ω prevents the generation of erroneous impulse due to noise, it makes difficult the detection of the incoming neurotransmitters. Therefore, P_b slightly

TABLE I
FIXED ARBITRARILY CHOSEN VALUES FOR CHANNEL PARAMETERS

τ_1	8	*Mean value of* d_i $(E[d_i])$	0.5
τ_2	10	*Variance of* d_i $(Var[d_i])$	1/64
T_{n+1}	100	*Total variance of synaptic noise* (V_T)	0.3
T_n	0	$P(q=1)$	0.8
Total number of affected AMPA receptors (g)	25	$P(q=0)$	0.2
Total number of affected receptors (j)	30	ω	5

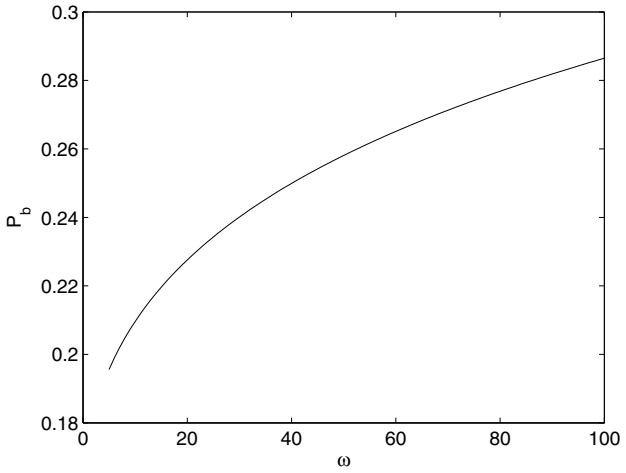

Fig. 9. The effect of ω on the channel performance with $r_k = 0.8$.

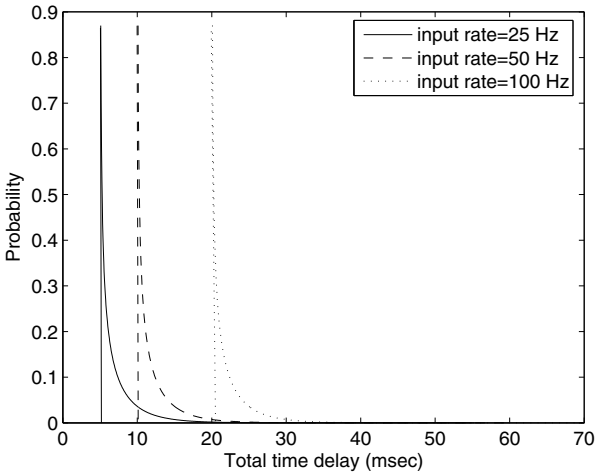

Fig. 11. Probability density function of total time delay.

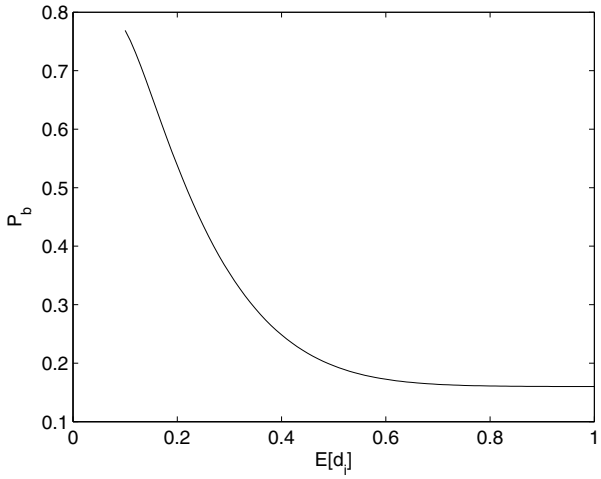

Fig. 10. The effect of expected value of the d_i on the channel performance with $r_k = 0.8$.

increases with ω. This result is supported by an experimental study in [24] which shows the same error behavior for higher threshold values.

The expected value of the d_i has the response as in Fig. 10. An increase in $E[d_i]$ yields the reduction in amplitude distortion. Therefore, P_b has a sharp decline, when $E[d_i]$ gets closer to 1.

The overall P_b may seem higher because of the smaller number of receptors, the low release probability and the low amplification due to the deactivation of NMDA receptors. However, these parameters are chosen arbitrarily, because they are not known exactly in the neuro-physiology. Therefore, P_b may be decreased easily by changing these values. However, the important point is to characterize P_b with these parameters rather than the actual values of P_b.

B. The Channel Delay

Before exciting an impulse at the output neuron in response to an input, each impulse is subject to the delay in time. The delay is found using (1) and random diffusion time whose probability density function is illustrated in (9) where b is taken as 1.

The channel delay is observed for different incoming input rates to the presynaptic terminal. The probability density function of the total time delay for them is shown in Fig. 11. According to that, higher input frequency increases the axonal propagation delay which perfectly matches the outcome of the experiment in [18]. This leads to rise in the total delay.

VIII. CONCLUSION

The properties of the neuro-spike communications are quite different than the traditional communication. For this reason, a lot of study and design paradigms are needed to set forth a complete understanding from the communication theory perspective. In this work, the neuro-spike channel between one input and output neuron at the CA region is characterized and analyzed.

The analysis reveals that an efficient communication can be obtained for low incoming signal rate to the presynaptic

terminal, higher number of NMDA receptors at the output and low synaptic noise. Moreover, having smaller threshold value and higher expected value of the random variable contribute to the channel performance. Furthermore, input frequency must be lower to have a smaller time delay. The serious brain diseases may be highly related with these parameters, and it may be helpful to observe these relations of the neuro-spike communications while seeking medical treatment.

We propose that this realistic model can be used as a new bio-inspired physical channel for nanonetworks. Our ongoing works are to develop appropriate protocols for this channel in order to realize a complete artificial neuro-inspired nanonetwork architecture.

REFERENCES

[1] I. F. Akyildiz, F. Brunetti, and C. Blazquez, "NanoNetworking: a new communication paradigm," *Comput. Netw. J. (Elsevier)*, June 2008.

[2] J. M. Bekkers, G. B. Richerson, and C. F. Stevens, "Origin of variability in quanta1 size in cultured hippocampal neurons and hippocampal slices," *Proc. Natl. Acad Sci. USA,* vol. 87, pp. 5359–5362, July 1990.

[3] J. M. Bekkers and C. F. Stevens, "Quantal analysis of EPSCs recorded from small numbers of synapses in hippocampal cultures," *J. Neurophysiology,* vol. 73, no. 3, pp. 1145–1156, Mar. 1995.

[4] P. Dayan and L. F. Abbott, *Neuroscience: Computational and Mathematical Modeling of Neural Systems*. MIT Press, 2001.

[5] L. J. DeFelice, *Introduction to Membrane Noise*. Plenum Press, 1981.

[6] L. E. Dobrunz and C. F. Stevens, "Heterogeneity of release probability, facilitation, and depletion at central synapses," *Neuron,* vol. 18, pp. 995–1008, June 1997.

[7] A. Enomoto, M. Moore, T. Nakano, *et al.*, "A molecular communication system using a network of cytoskeletal filaments," in *Proc. 2006 NSTI Nanotechnology Conf.*

[8] A. A. Faisal and S. B. Laughlin, "Stochastic simulations on the reliability of action potential propagation in thin axons," *PLoS Computational Biology,* vol. 3, no. 5, e79, May 2007.

[9] A. A. Faisal, L. P. J. Selen and D. M. Wolpert, "Noise in the nervous system," *Nature,* vol. 9, Apr. 2008.

[10] L. P. Gine and I. F. Akyildiz, "Molecular communication options for long range nanonetworks," *Comput. Netw. (Elsevier),* vol. 53, no. 16, pp. 2753–2766, Nov. 2009.

[11] A. Guney, B. Atakan, and O. B. Akan, "Mobile ad hoc nanonetworks with collision-based molecular communication," *IEEE Trans. Mobile Comput.,* vol. 11, no. 3, pp. 353–366, Mar. 2012.

[12] S. Hiyama, Y. Moritani, T. Suda, R. Egashira, A. Enomoto, M. Moore, and T. Nakano, "Molecular communication," in *Proc. 2005 NSTI Nanotechnology Conf.*

[13] A. Manwani, "Information-theoretic analysis of neuronal communication," Ph.D. dissertation, California Institute of Technology, Pasadena, CA, 2000.

[14] H. Markram, J. Lubke, M. Frotscher, A. Roth, and B. Sakmann, "Physiology and anatomy of synaptic connections between thick tufted pyramidal neurones in the developing rat neocortex," *J. Physiology,* vol. 500.2, pp. 409-440, 1997.

[15] T. Nakano, T. Suda, M. Moore, R. Egashira, A. Enomoto, and K. Arima, "Molecular communication for nanomachines using intercellular calcium signaling," in *Proc. 2005 IEEE Conf. Nanotechnology*.

[16] J. P. Meeks and S. Mennerick, "Action potential initiation and propagation in CA3 pyramidal axons," *J. Neurophysiology,* vol. 97, pp. 3460-3472, May 2007.

[17] M. Pierobon and I. F. Akyildiz, "A physical channel model for molecular communicationin nanonetworks," *IEEE J. Sel. Areas Commun.,* vol. 28, no. 4, May 2010.

[18] M. Raastad and G. M. G. Shepherd, "Single axon action potentials in the rat hippocampal cortex," *J. Physiology,* vol. 548.3, pp. 745–752, 2003.

[19] W. Rall, "Distinguishing theoretical synaptic potentials computed for different some-dendritic distributions of synaptic inputs," *J. Neurophysiology,* vol. 30, pp. 1138–1168, 1967.

[20] T. Schikorski and C. F. Stevens, "Quantitative ultrastructural analysis of hippocampal excitatory synapses," *J. Neuroscience,* vol. 17, no. 15, pp. 5858-5867, Aug. 1997.

[21] C. F. Stevens and Y. Wang, "Facilitation and depression at single central synapses," *Neuron 14,* vol. 14, pp. 795-802, Apr. 1995.

[22] A. J. Goldsmith and P. P. Varaiya, "Capacity, mutual information, and coding for finite-state Markov channels," *IEEE Trans. Inf. Theory*, vol. 42, pp. 868–886, May 1996.

[23] A. Kirkwood, S. M. Dudek, J. T. Gold, C. D. Aizenman, and M. F. Bear, "Common forms of synaptic plasticity in the hippocampus and neocortex in vitro," *Science*, vol. 260, June 1993.

[24] F. Franke, M. Natora, C. Boucsein, M. H. J. Munk, and K. Obermayer, "An online spike detection and spike classification algorithm capable of instantaneous resolution of overlapping spikes," *J. Comput. Neurosci,* vol. 29, pp. 127-148, 2010.

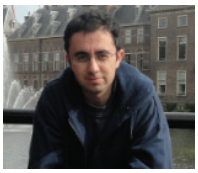

Eren Balevi received the B.S. and M.S. degrees in electrical and electronics engineering from Middle East Technical University, Ankara, Turkey, in 2008 and 2010 respectively. He is currenly pursuing the Ph.D. degree at the same department of Middle East Technical University, Ankara, Turkey. His current research interests are in the general areas of nanoscale communications, multi-user wireless communications, and signal processing.

Ozgur B. Akan [M00, SM07] (akan@ku.edu.tr) received his Ph.D. degree in electrical and computer engineering from the Broadband and Wireless Networking Laboratory, School of Electrical and Computer Engineering, Georgia Institute of Technology in 2004. He is currently a full professor with the Department of Electrical and Electronics Engineering, Koc University and the director of the Next-generation and Wireless Communications Laboratory. His current research interests are in wireless communications, nano-scale and molecular communications, and information theory. He is an Associate Editor of IEEE TRANSACTIONS ON VEHICULAR TECHNOLOGY, *International Journal of Communication Systems* (Wiley), and *Nano Communication Networks Journal* (Elsevier).